limiting spectrum of the reduced form (Figure 3a) can be produced and then quantitatively oxidized back to $Re^{V}$. For *trans*-$PhNRe^{V}(bpy)_2(OEt)^{2+}$, reduction on our spectroelectrochemical time scale (each scan in Figure 3a is made in ca. 5 s) produces predominantly *trans*-$PhNRe^{IV}(bpy)_2(OEt)^{+}$; however, a slow chemical process drains this away to product. This is evidenced by the appearance of a new oxidative process at −0.05 V (Figure 3b) and the observation that reoxidation of $PhNRe^{IV}(bpy)_2(OEt)^{+}$ immediately after spectroelectrochemical reduction regenerates the limiting spectrum of *trans*-$PhNRe^{V}(bpy)_2(OEt)^{2+}$ mixed with the spectral signature of a new complex (not shown in Figure 3b). In the oxidative branch of the cyclic voltammogram, only *trans*-$PhNRe^{V}(bpy)_2(OEt)^{2+}$ is observed to be redox-active, exhibiting a single-electron oxidation ($E_p$ = ca. +1.95 V; feature d in Figure 3b), which generates a transiently stable *trans*-$PhNRe(bpy)_2(OEt)^{3+}$ species that is coupled to the rapid formation of a new complex ($E_p$ = ca. +1.02 V; feature e in Figure 3b).

The observation of trans bpy ligands which are apparently stabilized by strong multiple bonding in a $Re^{V}$–imido complex, coupled with a rich redox chemistry of a presumed $Re^{VI}$ state and an observed $Re^{IV}$ state, will enable us to define the interplay of steric and electronic requirements that exist in the high-valent polypyridine chemistry of rhenium.

We have been unsuccessful in our attempts to convert *trans*-$PhNRe(bpy)_2(OEt)^{2+}$ to its cis isomer. Extended heating at reflux (48 h) in EtOH results in no apparent reaction. This is consistent with either the trans form being the thermodynamic product or an abnormally high activation free energy for trans to cis isomerization. Protonation under mild conditions proceeds through a green intermediate, which eventually loses bpy and generates *mer*-$PhNRe(bpy)Cl_3$ in quantitative yield, presumably as depicted in eq 5.

$$\textit{trans}\text{-}PhNRe(bpy)_2(OEt)^{2+} + 3HCl \xrightarrow{EtOH,\ \Delta} \textit{mer}\text{-}PhNRe(bpy)Cl_3 + bpyH^{+} + EtOH + H^{+} \quad (5)$$

The unusual stability of *trans*-$PhNRe(bpy)_2(OEt)^{2+}$ can be rationalized in terms of a qualitative molecular orbital argument,[16] which predicts enhanced stability of the 18-$e^{-}$ trans isomer for the model complex *trans*-$O_2Mo(PH_3)_4$, relative to the cis form. In our example, the electronic stabilization of multiple bonding apparently overcomes the steric hindrance imposed by the "bumping" of the 6, 6′ protons on the bpy ligand. Because of this electronic stabilization, it seems likely that an extended series of abnormally stable trans complexes with axial metal–ligand multiple bonds can be prepared: for example, *trans*-$O_2Re(bpy)_2^{+}$, *trans*-$NRe(bpy)_2(OR)^{+}$, and *trans*-$ORe(bpy)_2(OR)^{2+}$.

**Acknowledgment.** We thank the National Science Foundation for support under the EPSCoR Program and the University of Wyoming for a Basic Research Grant.

**Registry No.** *trans,mer*-$PhNRe(PPh_3)_2Cl_3$, 62192-31-8; *mer*-$PhNRe(bpy)Cl_3$, 139199-31-8; *trans*-$[Re(NPh)(Cl)(dppe)_2](PF_6)_2$, 139199-33-0; *trans*-$[Re(NPh)(OEt)(bpy)_2](PF_6)_2$, 139199-35-2; *trans*-$[PhNRe(dppe)_2Cl]^{+}$, 139199-36-3; *trans*-$[PhNRe(bpy)_2(OEt)]^{+}$, 139199-37-4.

**Supplementary Material Available:** For *trans*-$[PhNRe(bpy)_2(OEt)](PF_6)_2$, tables of atomic coordinates and isotropic displacement coefficients (Table 1), bond lengths (Table 2), bond angles (Table 3), anisotropic displacement coefficients (Table 4), hydrogen coordinates and isotropic displacement coefficients (Table 5), crystallographic data collection parameters (Table 6), and solution and refinement parameters (Table 7) (7 pages); a listing of observed and calculated structure factors (21 pages). Ordering information is given on any current masthead page.

(16) Mingos, D. M. P. *J. Organomet. Chem.* **1979**, *179*, C29.

Department of Chemistry
University of Wyoming
Laramie, Wyoming 82071-3838

**Mohammed Bakir**
**Scott Paulson**
**Patricia Goodson**
**B. Patrick Sullivan***

*Received October 4, 1991*

# Articles

Contribution from the Department of Chemistry and Biochemistry, The University of Texas at Austin, Austin, Texas 78712

## Electrochemical Investigation of the Association of Distamycin A with the Manganese(III) Complex of *meso*-Tetrakis(*N*-methyl-4-pyridiniumyl)porphine and the Interaction of This Complex with DNA

Marisol Rodriguez and Allen J. Bard*

*Received July 26, 1991*

Differential pulse voltammetry (DPV) was used to study the interaction of distamycin A (Dis) with the manganese(III) complex of *meso*-tetrakis(*N*-methyl-4-pyridiniumyl)porphine ($Mn^{III}P$) and that of this complex with calf thymus (CT) DNA. The addition of distamycin to $Mn^{III}$ caused a diminution in the peak current and a positive shift in the peak potential of the DPV wave for the reduction of $Mn^{III}P$. This effect on the peak current is a result of a decrease in the diffusion coefficient ($D$) of $Mn^{III}P$ from $D_f = 1.2\ (\pm 0.3) \times 10^{-6}$ cm$^2$/s to $D_b = 7.2\ (\pm 0.2) \times 10^{-8}$ cm$^2$/s. An amperometric titration was used to show that two distamycins bind to one $Mn^{III}P$ with an overall binding constant of $K = 5\ (\pm 3) \times 10^{8}$ $M^{-2}$, assuming a static equilibrium model, probably by axial coordination of the oxygen atom of the formyl end of Dis to Mn(III). The 23-mV positive shift in the DPV peak potential of $Mn^{III}P$ indicates that distamycin binds 2.5 times more strongly to $Mn^{II}P$ than to $Mn^{III}P$. The $Mn^{III}P(Dis)_2$ complex interacts with sonicated CT DNA; DPV and amperometric titration were also used to investigate this interaction.

### Introduction

In this work we describe the association of the manganese(III) complex of *meso*-tetrakis(*N*-methyl-4-pyridiniumyl)porphine ($Mn^{III}P$) and distamycin A (Dis) (Figure 1) in the absence and in the presence of sonicated calf thymus (CT) DNA. Both $Mn^{III}P$ and Dis are known to bind individually to DNA. We originally intended to study the interaction of DNA with Dis by electrochemical competition experiments with electroactive $Mn^{III}P$ using differential pulse voltammetry (DPV).[1] Dis is not electroactive in the potential range where Mn(III) is reduced, but it can be irreversibly oxidized at 0.8 V vs SCE. However, we found that

(1) Rodriguez, M.; Kodadek, T.; Torres, M.; Bard, A. J. *Bioconjugate Chem.* **1990**, *1*, 123.

0020-1669/92/1331-1129$03.00/0 

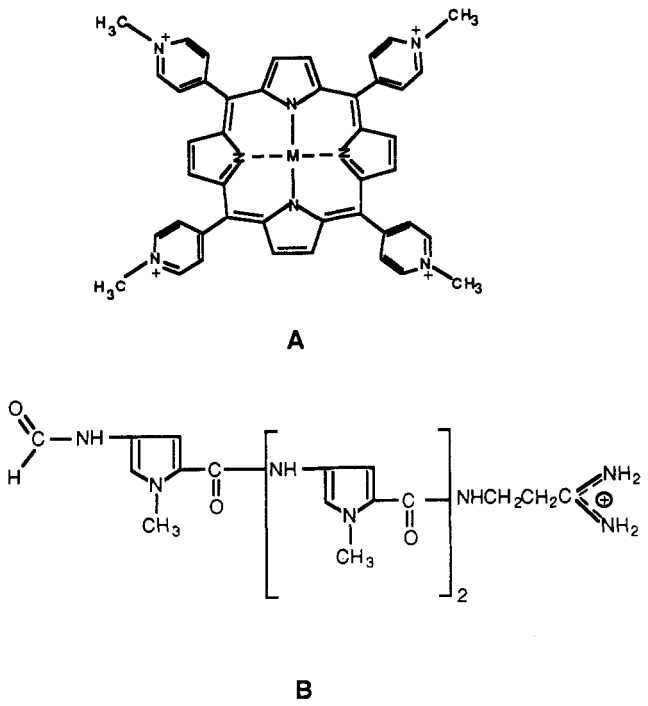


**Figure 1.** Structure of (A) $Mn^{III}P$ and (B) distamycin A.

Dis associates strongly with $Mn^{III}P$ and that DPV could be used to study this interaction, as well as the binding of the complex with DNA.

Distamycin A is an oligopeptide antibiotic with antitumor and antiviral activity[2,3] but is best known as an inhibitor of biological processes; for example, its binding to RNA polymerase inhibits transcription in vitro.[2] Distamycin binds to DNA within the minor groove at A-T rich sequences.[2-6] The amide groups in the oligopeptide form bifurcated bonds to N(3) of adenine or the O(2) of thymine in adjacent bases on opposite strands.[7] The binding site size of Dis on DNA has been reported to be in the range 4–6 base pairs.[8-11] Studies of the binding of distamycin with DNA have been done using footprinting,[12] affinity cleaving methods,[9,10] dichroism studies,[8,13] NMR,[14] X-ray,[7] and calorimetry.[15]

$Mn^{III}P$ was used to study the binding of a related oligopeptide, netropsin, to DNA by footprinting;[16,17] however, no interaction between these two species in the absence of DNA was reported. In that work the ability of $Mn^{II}P$ to cleave DNA was employed to obtain information about the binding of the oligopeptide to DNA.

In this paper we report the binding of distamycin to $Mn^{III}P$, and we discuss the implications of this complexation and its binding to DNA in comparison with that of $Mn^{III}P$.

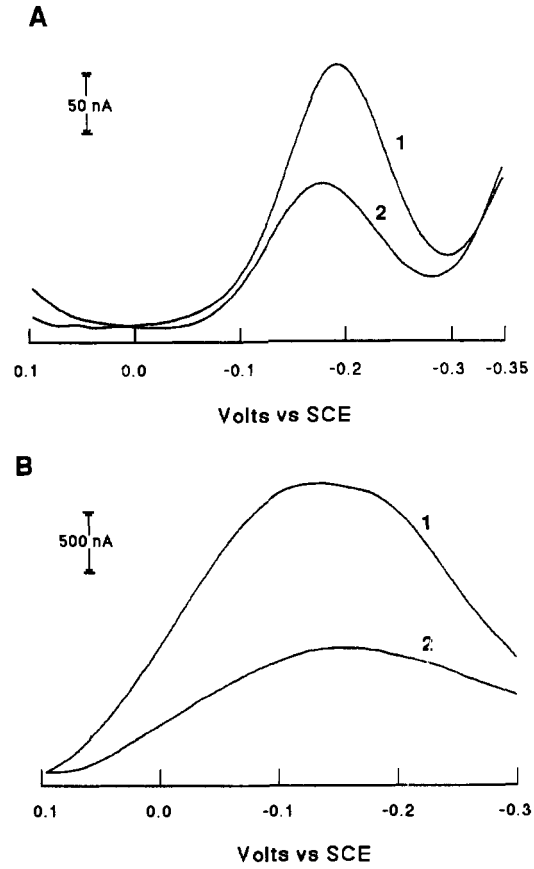


**Figure 2.** Differential pulse voltammograms of 0.1 mM $Mn^{III}P$ in 5 mM Tris-HCl, 50 mM NaCl, pH 7, in the (1) absence and (2) presence of 0.2 mM distamycin A: (A) solutions deaerated with nitrogen; (B) solutions saturated with $O_2$. (Note current scale in (B) is 10 times that in (A).)

## Experimental Section

The manganese(III) complex of *meso*-tetrakis(*N*-methyl-4-pyridiniumyl)porphine was prepared as the perchlorate salt by the procedure of Pasternack et al.[18] The metalloporphyrin was dissolved in 5 mM Tris-HCl, 50 mM NaCl buffer, pH 7, and its concentration was determined spectrophotometrically with $\epsilon_{463} = 0.92 \times 10^5\ M^{-1}\ cm^{-1}$.[18] Distamycin A [Figure 1B; [1-methyl-4-[1-methyl-4-[1-methyl-4-(formylamino)pyrrole-2-carboxamido]pyrrole-2-carboxamido]pyrrole-2-carboxamido]propionamidine] and calf thymus (CT) DNA were purchased from Sigma Chemical Co. (St. Louis, MO) and were used without further purification. Distamycin concentrations were determined by UV absorbance using $\epsilon_{303} = 2.4 \times 10^4\ M^{-1}\ cm^{-1}$.[14] Solutions were used immediately after preparation, since distamycin is unstable in the buffer over a period of days. DNA solutions were prepared and sonicated as described earlier.[1] Concentrations of CT DNA are expressed in terms of nucleotide phosphate concentration, [NP]. 3,5-Dimethylpyrazole-1-carboxamidine nitrate (DMPCA) was obtained from Aldrich Chemical Co. (Milwaukee, WI), and *N*,*N*-dimethylformamide (DMF), from J. T. Baker (Phillipsburg, NJ); both were used as received. All other chemicals were reagent grade and were used as received. Solutions were prepared with deionized water from a Millipore Milli-Q system.

Voltammetric studies were performed using a Bioanalytical Systems (BAS-100) electrochemical analyzer. Differential pulse voltammetric (DPV) experiments were done with the following parameters: pulse amplitude (PA), −50 mV; pulse width, 500 ms; sweep rate ($v$), 4 mV/s; sample width, 166 ms; pulse period, 1 s. Voltammetric studies were carried out as described previously,[1] with a Pt disk (area, 0.026 $cm^2$) working electrode, a Pt flag counter electrode, and a saturated calomel

(2) Zimmer, C.; Wähnert, U. *Prog. Biophys. Mol. Biol.* **1986**, *47*, 31.
(3) Gale, E. F.; Cundlifle, E.; Reynolds, P. E.; Richmond, M. H.; Waring, M. J. *The Molecular Basis of Antibiotic Action*, 2nd ed.; Wiley: London, 1981; pp 258–401.
(4) Fox, K. R.; Waring, M. J. *Nucleic Acids Res.* **1984**, *12*, 9271.
(5) Lane, M. J.; Dabrowiak, J. C.; Vournakis, J. N. *Proc. Natl. Acad. Sci. U.S.A.* **1983**, *80*, 3260.
(6) Van Dyke, M. W.; Hertzberg, R. P.; Dervan, P. B. *Proc. Natl. Acad. Sci. U.S.A.* **1982**, *79*, 5470.
(7) Coll, M.; Frederick, C. A.; Wang, A. H.-J.; Rich, A. *Proc. Natl. Acad. Sci. U.S.A.* **1987**, *84*, 8385.
(8) Arcamone, F. *Bio-Organic Heterocycles-Synthesis, Mechanism and Bioactivity*; Elsevier: Amsterdam, 1986; pp 119–134.
(9) Schultz, P. G.; Dervan, P. B. *J. Biomol. Struct. Dyn.* **1984**, *1*, 1133.
(10) Taylor, J. S.; Schultz, P. G.; Dervan, P. B. *Tetrahedron* **1984**, *40*, 457.
(11) Uchida, K.; Pyle, A. M.; Morii, T.; Barton, J. K. *Nucleic Acid Res.* **1989**, *17*, 10259.
(12) Fish, L.; Lane, M. J.; Vournakis, S. N. *Biochemistry* **1988**, *27*, 6026.
(13) Dattagupta, N.; Hogan, M.; Crothers, D. M. *Biochemistry* **1980**, *19*, 5998.
(14) Pelton, J. G.; Wemmer, D. E. *J. Am. Chem. Soc.* **1990**, *112*, 1393.
(15) Breslauer, K. J.; Remeta, D. P.; Chou, W.-Y.; Fenante, R.; Curry, J.; Zaunczkowski, D.; Snyder, J. G.; Marky, L. A. *Proc. Natl. Acad. Sci. U.S.A.* **1987**, *84*, 8922.
(16) Ward, B.; Rehfuss, R.; Dabrowiak, J. C. *J. Biomol. Struct. Dyn.* **1987**, *4*, 685.
(17) Ward, B.; Rehfuss, R.; Goodisman, J.; Dabrowiak, J. C. *Biochemistry* **1988**, *27*, 1198.
(18) Pasternack, R. F.; Gibbs, E. J.; Villafranca, J. J. *Biochemistry* **1983**, *22*, 2406.

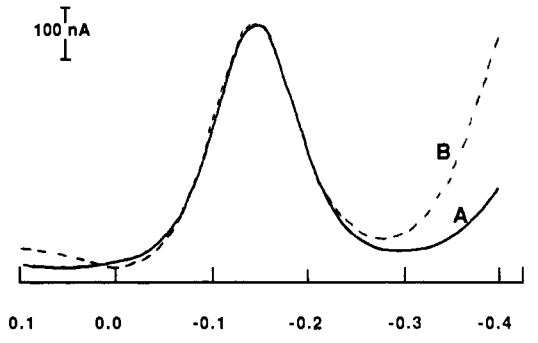


**Figure 3.** Differential pulse voltammograms of 0.1 mM $Ru(NH_3)_6^{3+}$ in 5 mM Tris-HCl, 50 mM NaCl, pH 7, in the (A) absence and (B) presence of 0.4 mM distamycin A.

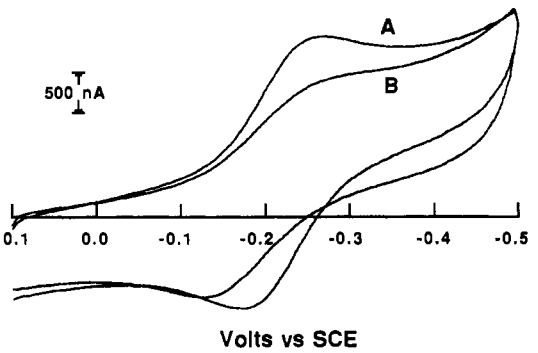


**Figure 4.** Cyclic voltammograms of 0.5 mM $Mn^{III}P$ in 5 mM Tris-HCl, 50 mM NaCl, pH 7, in the absence (A) and (B) presence of 0.5 mM distamycin A (sweep rate 100 mV/s).

reference electrode (SCE). All studies were carried out in 5 mM Tris-HCl, 50 mM NaCl, pH 7. Solutions were deoxygenated with nitrogen, unless otherwise specified.

Ultraviolet-visible absorption spectra were obtained using a Hewlett-Packard 8451A diode-array spectrophotometer.

## Results

**Voltammetric Studies of the Interaction of $Mn^{III}P$ with Distamycin.** Differential pulse voltammograms (DPV) of the reduction of 0.1 mM $Mn^{III}P$ in the absence of oxygen, with and without Dis, are shown in Figure 2A. The change of the voltammetric response—a decrease in the peak current ($I_p$) and shift of the peak potential ($E_p$)—demonstrates the interaction between these two species. Since $Mn^{II}P$ reacts with oxygen,[1] $I_p$ during the reduction of $Mn^{III}P$ is enhanced in a solution containing dissolved oxygen (a catalytic or EC′ electrode reaction scheme).[19] The binding of Dis to $Mn^{III}P$ also inhibited the catalytic reduction of $O_2$ by $Mn^{II}P$ (Figure 2B). A similar inhibition by methylimidazole bound axially to the Mn(III) complex of tetraphenylporphine (TPP) has been reported.[20]

To ensure that the decrease in $I_p$ by the addition of Dis was not caused by blockage of the electrode surface through adsorption of Dis, DPV of $Ru(NH_3)_6^{3+}$ was carried out in the absence and presence of Dis. The ruthenium compound, which is reduced at potentials similar to those for $Mn^{III}P$, is positively charged but, unlike $Mn^{III}P$, which has two axially bound water molecules,[21] contains six nonlabile ligands and is not expected to interact with Dis. The electrochemical behavior of the ruthenium compound was not affected by the addition of Dis (Figure 3), eliminating the passivation of the electrode by Dis and supporting the association of Dis and $Mn^{III}P$ as the cause for the decrease in $I_p$ shown in Figure 2A.

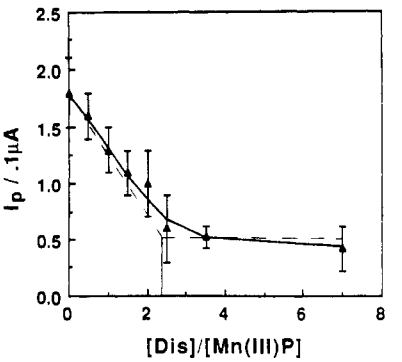


**Figure 5.** Titration of 0.1 mM $Mn^{III}P$ with distamycin A. Points represent experimental data, with the scatter estimated, and the solid line represents the curve for the averaged binding constant given in Table I assuming static equilibria. Error bars correspond to $\pm 2\sigma$ for three measurements. The two straight lines shown were used to approximate the stoichiometry of the complex formed between $Mn^{III}P$ and distamycin A.

**Table I.** Determination of the Overall Binding Constant for $Mn^{III}P(Dis)_2$ for Static and Mobile Equilibria Models

| [Dis]/[$Mn^{III}P$] | $K/10^8$ $M^{-2}$ (static) | $K/10^9$ $M^{-2}$ (mobile) |
|---|---|---|
| 0 | | |
| 0.5 | 3.08 | 2.90 |
| 1.0 | 6.69 | 688[a] |
| 1.5 | 4.13 | 5.19 |
| 2.0 | 1.89 | 0.87 |
| 2.5 | 11.3 | 3.95 |
| 3.5 | 4.70 | 1.27 |
| 7.0 | | |
| $K_{av}$[b] | 5 (±3) | 3 (±2) |

[a] This value is larger because coincidentally the concentration of complex calculated from the peak current is close to half the concentration of Dis added, so that the concentration of free Dis at this point is calculated to be very low. Under these conditions the concentration of free Dis, and hence $K$, is very sensitive to small errors in the $I_p$ value. For this reason, the $K$ at this point was not used for the evaluation of the averaged binding constant ($K_{av}$). [b] Values in parentheses are standard deviations of $K$.

DPV was used as the electrochemical method in these studies, because it was more suitable for the low concentrations of $Mn^{III}P$ and Dis employed. However, to ensure that the observed effect was not method-related (e.g., because of kinetic limitations), cyclic voltammetry was also applied. Cyclic voltammograms (CV) of 0.5 mM $Mn^{III}P$ in the absence (A) and in the presence of 0.5 mM distamycin (B) are shown in Figure 4. The cyclic voltammetric behavior of $Mn^{III}P$ is characterized by a quasireversible behavior ($\Delta E_p \approx 85$ mV in the absence of distamycin and $\Delta E_p \approx 110$ mV in the presence of distamycin) and the same decrease of peak current (here superimposed on the charging and background current) on addition of Dis. Thus, the current at the DPV peak can be ascribed to a quasireversible electron-transfer reaction, and the decrease seen in DPV is not due to kinetic complications.

The stoichiometry and the overall binding constant for the complex formed between $Mn^{III}P$ and Dis was determined by amperometric titration (i.e., measurement of $I_p$ with addition of Dis) (Figure 5), analogous to the approach previously used to study the interaction of metal complexes with DNA.[22-24] In the titration curve, the decrease of the peak current with addition of Dis occurs as a result of the diminution of the diffusion coefficient of the metalloporphyrin when it is bound to Dis ($D_b$). The diffusion coefficient of the free metalloporphyrin, $D_f = 1.2\ (\pm 0.3) \times 10^{-6}$ $cm^2/s$, decreased to $D_b = 7.2\ (\pm 0.2) \times 10^{-8}$ $cm^2/s$ when

(19) Bard, A. J.; Faulkner, L. R. *Electrochemical Methods*; Wiley: New York, 1980; pp 429-487.
(20) Creager, S. E.; Murray, R. W. *Inorg. Chem.* **1987**, *26*, 2612.
(21) Harriman, A.; Porter, G. *J. Chem. Soc., Faraday Trans. 2* **1979**, *75*, 1532.
(22) Carter, M. T.; Bard, A. J. *J. Am. Chem. Soc.* **1987**, *109*, 7528.
(23) Carter, M. T.; Rodriguez, M.; Bard, A. J. *J. Am. Chem. Soc.* **1989**, *111*, 8901.
(24) Rodriguez, M.; Bard, A. J. *Anal. Chem.* **1990**, *62*, 2658.

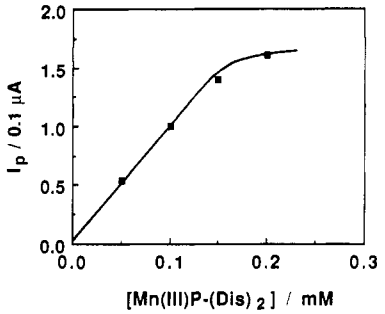


**Figure 6.** DPV peak current as a function of the concentration of $Mn^{III}P(Dis)_2$. Solutions contained [Dis]/[$Mn^{III}P$] = 2 in 5 mM Tris-HCl, 50 mM NaCl, pH 7.

[Dis]/[$Mn^{III}P$] = 7, where brackets are used to indicate total (analytical) concentrations of species. By extrapolation of the points in Figure 5 for the early and late parts of the titration curve, the $Mn^{III}P$:Dis stoichiometric ratio was found to be about 1:2, so that the interaction can be given as

$$Mn^{III}P + 2Dis \overset{K}{\rightleftharpoons} Mn^{III}P(Dis)_2 \qquad (1)$$

The overall binding constant ($K$) was calculated individually at every point along the titration and averaged assuming either a static or mobile equilibrium;[23] the values obtained are summarized in Table I. The experimental values of the concentration of bound and free $Mn^{III}P$ were initially obtained from the expression of the DPV peak current ($I_p$; eq 2) and the binding constant was determined using eq 3.

For our experimental conditions, $I_p$ is defined as

$$I_p = 1567 C_0 D^{1/2} \qquad (2)$$

and

$$D = (D_f^{1/2} X_f + D_b^{1/2} X_b)^2$$

assuming static equilibria or

$$D = D_b X_b + D_f X_f$$

assuming mobile equilibria, where $C_0$ is the total concentration of $Mn^{III}P$ and $X_f$ and $X_b$ are mole fractions of free and bound $Mn^{III}P$, respectively.

$$K = \frac{(Mn^{III}P(Dis)_2)}{(Mn^{III}P)(Dis)^2} \qquad (3)$$

Although the values for $K$ showed some scatter, especially for the mobile equilibrium model, the method provided a good estimate of the magnitude of the interaction. The solid line in Figure 5 represents the titration curve for $K = 5.3 \times 10^8$ $M^{-2}$ (assuming static equilibrium). To ensure that the peak current ($I_p$) was proportional to the concentration of $Mn^{III}P$ in the range of concentrations used in the titration, and in later studies of the interaction of $Mn^{III}P(Dis)_2$ with DNA, DPV of solutions of $Mn^{III}P$ and Dis of different concentrations, with [Dis]/[$Mn^{III}P$] = 2, was carried out. $I_p$ was linear with concentration of $Mn^{III}P(Dis)_2$ over the range 0–0.15 mM (Figure 6). Above 0.15 mM the curve leveled off, suggesting that this concentration represents the solubility of this species in this buffer solution. This calibration curve defines the valid range of concentrations that can be used to study the interaction of this complex with DNA.

The addition of distamycin also caused some shift in the DPV peak potential ($E_p$) of $Mn^{III}P$ (Figure 7). The $E_p$ value observed for the free metalloporphyrin, $E_p = -185$ (±5) mV, was slightly more negative (by 10 mV) than that reported in our earlier publication,[1] probably due to a small change in the experimental conditions. After addition of 0.7 mM Dis, $E_p$ of $Mn^{III}P$ was −162 (±8) mV.

To determine which atom or group of atoms of distamycin are involved in the binding to the Mn center, we performed DPV experiments of $Mn^{III}P$ in the presence of two different compounds, each one containing one of the terminal groups of distamycin (a formyl group or an amidine group). To test if the amidine group reacts with the metalloporphyrin, we carried out the DPV of 0.1 mM $Mn^{III}P$ with an excess of 3,5-dimethylpyrazole-1-carboxamidine (DMPCA). As shown in Figure 8B, no change was observed in the DPV of $Mn^{III}P$ indicating that DMPCA does not coordinate to $Mn^{III}P$ and the amidine moiety is probably not responsible for distamycin interaction. Addition of 0.4 mM *N,N*-dimethylformamide (DMF) to 0.1 mM $Mn^{III}P$ caused a shift in the $E_p$ of $Mn^{III}P$ from −188 to −168 (Figure 8C). This +20-mV shift in $E_p$, which resembles that observed for $Mn^{III}P$ in the presence of distamycin, suggests that it is the formyl group of Dis that interacts with $Mn^{III}P$. No decrease in the peak current is expected with DMF, because DMF is a small molecule and its addition does not decrease the diffusion coefficient of $Mn^{III}P$. Isolation and characterization of a similar complex, $Mn^{III}TPP(DMF)_2$ (where TPP = tetraphenylporphyrin), have been reported.[25] X-ray crystallographic analysis of that complex indicated that the DMF oxygen atom coordinates axially to the Mn(III) atom.

The structure of the $Mn^{III}P(Dis)_2$ complex was not determined, since we did not succeed in our attempt to grow crystals for crystallographic studies.

For a system where a metal, M, in its reduced and oxidized form is bound to a ligand, L, and they exist predominantly complexed, the reaction at the electrode can be described as follows:

$$ML_x^{m+} + ne^- \rightleftarrows ML_y^{(m-n)} + (x - y)L \qquad (4)$$

Here $n$ is the number of electrons involved in the redox process

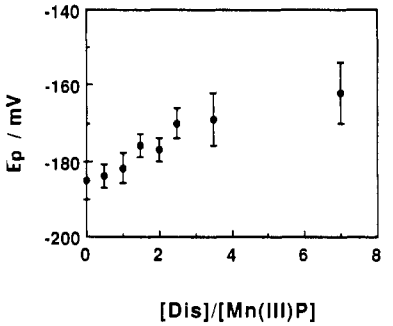


**Figure 7.** Dependence of DPV peak potential of $Mn^{III}P$ on the ratio of [Dis]/[$Mn^{III}P$]. Error bars correspond to ±2$\sigma$ for three measurements.

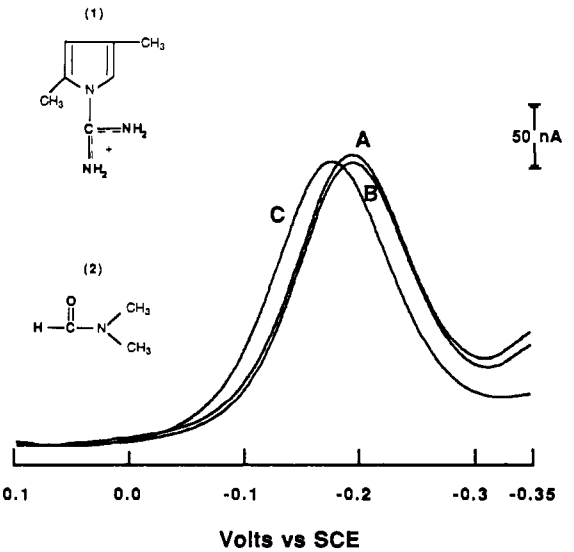


**Figure 8.** DPV of 0.1 mM $Mn^{III}P$ in 5 mM Tris-HCl, 50 mM NaCl, pH 7, (A) alone and in the presence of (B) 2.6 mM 3,5-dimethylpyrazole-1-carboxamidine (DMPCA) and (C) 0.4 mM dimethylformamide (DMF). Inset: Structure of (1) DMPCA and (2) DMF.

(25) Hill, C. L.; Williamson, M. M. *Inorg. Chem.* **1985**, *24*, 2836.

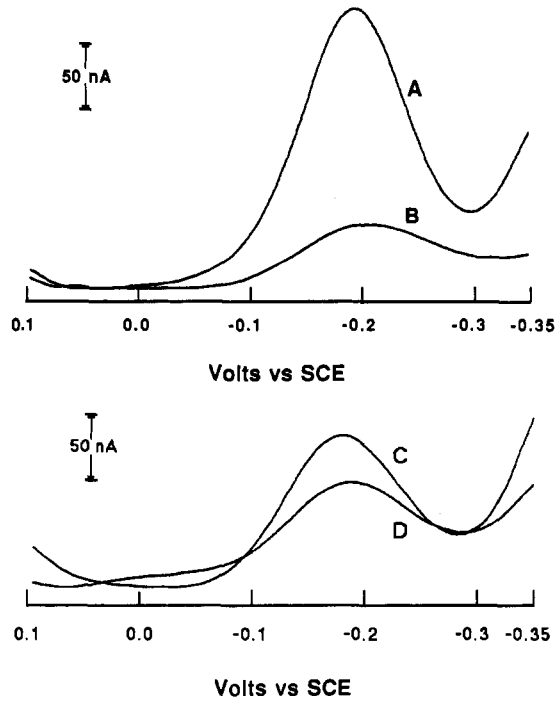


**Figure 9.** DPV of (A, B) 0.1 mM $Mn^{III}P$ and of (C, D) 0.1 mM $Mn^{III}P(Dis)_2$ (A, C) in the absence of DNA, (B) in the presence of 2.0 mM NP, and (D) in the presence of 2.6 mM NP. Buffer: 5 mM Tris-HCl, 50 mM NaCl, pH 7.

and $x$ and $y$ are the coordination numbers of the reduced and oxidized forms, respectively. The slope of a plot of the formal potential of the bound species, $E_b°'$, vs log ($L$) is equal to $-0.059(x - y)/n$, where the coordination of the reduced and oxidized complex can be evaluated.[26] The formal potentials can be evaluated from the peak potentials by inclusion of the pulse amplitude, PA, as shown in the expression[19]

$$E_{1/2} = E_p + PA/2 \quad (5)$$

and the ratios of the diffusion coefficients of free and bound $Mn^{II}P$ and $Mn^{III}P$. To be valid, such experiments should be performed using a large free ligand concentration. In this work we were not able to carry out such experiments because of the low solubility of Dis. However, in a separate experiment, with 0.15 mM $Mn^{III}P$ and solutions where $4 \leq [Dis]/[Mn^{III}P] < 7$, $E_p$ was essentially constant within the error of the measurements. The lack of change in $E_p$, and therefore in $E_b°'$, at low Dis concentrations suggests that the reduced form, $Mn^{II}P$, also binds two Dis molecules. Bis-ligated complexes of Mn(II) porphyrins have been reported in aqueous media; in nonaqueous solutions, only mono(ligand) complexes of Mn(II) have been observed.[27,28]

**Voltammetric Studies of the Interaction of $Mn^{III}P(Dis)_2$ with CT DNA.** The nature of the interaction of $Mn^{III}P(Dis)_2$ with DNA is especially interesting, since both $Mn^{III}P$ and Dis bind individually to DNA. We attempted to investigate the interaction of $Mn^{III}P(Dis)_2$ with sonicated CT DNA using the procedure previously reported.[1] This procedure involves measuring the DPV peak current associated with the reduction of the complex in the presence of different concentrations of DNA. The complex was initially formed by combining 0.1 mM $Mn^{III}P$ and 0.2 mM Dis. Figure 9 shows the effect of the addition of sonicated CT DNA on the DPV behavior of 0.1 mM $Mn^{III}P$ (A, B) and 0.1 mM $Mn^{III}P(Dis)_2$ (C, D). Figure 9A,B shows the large diminution of the peak current and the negative shift of the peak potential of $Mn^{III}P$ in the presence of DNA as reported previously.[1] In Figure 9C,D, a similar change was observed for $Mn^{III}P(Dis)_2$ but the effect was less pronounced, because the diffusion coefficient of $Mn^{III}P(Dis)_2$ is much smaller than that of $Mn^{III}P$, so the relative effect of binding with DNA on $D$ is smaller. Nevertheless, the diminution of $I_p$ for $Mn^{III}P(Dis)_2$ on adding DNA is sufficient to study the interaction with DNA. At higher DNA concentrations, the $I_p$ value is suppressed even more (Figure 10B).

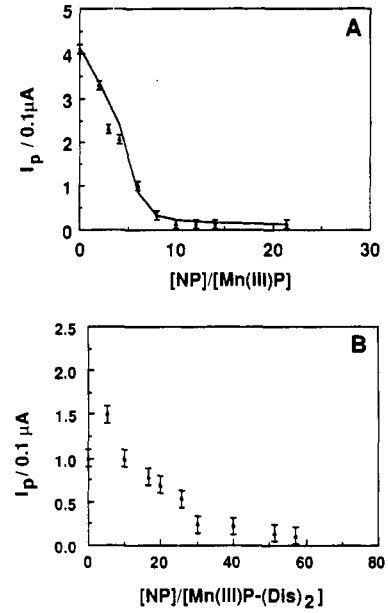


**Figure 10.** Titration of (A) 0.1 mM $Mn^{III}P$ and (B) 0.1 mM $Mn^{III}P(Dis)_2$ with sonicated CT DNA. Titration curve A, from ref 1, has a sample width = 17 ms and pulse width = 50 ms, and the working electrode was a Pt disk (area 0.023 $cm^2$). Error bars correspond to the average of $\pm 2\sigma$ for all the data points.

Figure 10 shows the titration of $Mn^{III}P$ (A) and of $Mn^{III}P(Dis)_2$ (B) with sonicated CT DNA. In Figure 10B the DPV peak current decreased for $R > 10$ (where $R = [NP]/[Mn^{III}P(Dis)_2]$) because the diffusion of $Mn^{III}P(Dis)_2$ is much slower when it is bound to DNA. However, at low DNA concentrations, for example, when $R = 5$, the $Mn^{III}P(Dis)_2$-DNA complex precipitated and the current was higher than for $Mn^{III}P(Dis)_2$ itself due to adsorption of $Mn^{III}P(Dis)_2$–DNA at the electrode surface. This effect of adsorption was verified by the DPV response of an electrode that was transferred from this solution (after continuous cycling between 0.1 and −0.4 V) to a solution of pure buffer, where a reduction wave of $Mn^{III}P(Dis)_2$–DNA adsorbed or precipitated on the electrode surface was seen. At higher DNA concentrations, the $Mn^{III}P(Dis)_2$ complex did not precipitate in the solution and addition of more DNA to a solution containing the precipitate caused it to dissolve.

We did not pursue a more quantitative treatment of the binding of $Mn^{III}P(Dis)_2$ to DNA because of this adsorption complication. Moreover, determination of the binding constant for a large molecule such as $Mn^{III}P(Dis)_2$ may require a method of analysis,[29] more complicated than that previously used,[22,23] which could account for overlapping of binding sites. The titration curve of $Mn^{III}P(Dis)_2$ with DNA (Figure 10B) shows that the point at which the current decreases to a fairly constant value (characteristic of binding of $Mn^{III}P(Dis)_2$) occurred at higher DNA concentrations than that found with $Mn^{III}P$ (Figure 10A). This is consistent with the expected larger binding site size for $Mn^{III}P(Dis)_2$ compared to $Mn^{III}P$. By extrapolation of the end point of the curve shown in Figure 10B, the binding site size was determined to be approximately 15 base pairs.

The changes in the DPV peak potential ($E_p$) of $Mn^{III}P(Dis)_2$ with DNA are shown in Figure 11. The peak potential of $Mn^{III}P(Dis)_2$, $E_p = -177$ (±4) mV, shifted to more positive values by 17 mV, when $R = 5$, but to more negative potentials at higher DNA concentrations. At $R = 57$, $E_p = -204$ (±4) mV.

(26) Kolthoff, I. M.; Lingane, J. J. *Polarography*, 2nd ed.; Interscience: New York, 1952; Vol. 1, pp 211–234.
(27) Boucher, L. J. *Coord. Chem. Rev.* **1972**, *7*, 289.
(28) Davis, D. G.; Montalvo, J. G. *Anal. Lett.* **1968**, *1*, 641.
(29) McGhee, J. D.; von Hippel, P. H. *J. Mol. Biol.* **1974**, *86*, 469.

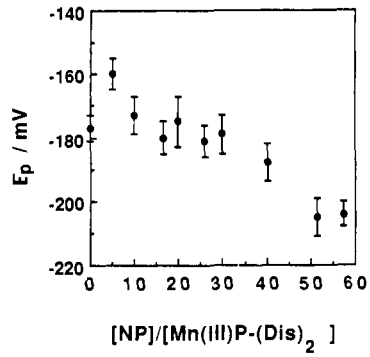


**Figure 11.** Effect of $R$ ([NP]/[$Mn^{III}P(Dis)_2$]) on the DPV peak potential $E_p$ of 0.1 mM $Mn^{III}P(Dis)_2$. Error bars correspond to the average of $\pm 2\sigma$ for all the data points.

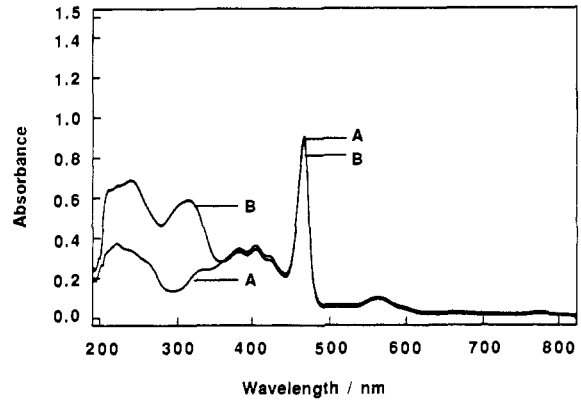


**Figure 12.** Visible spectra of (A) 9 $\mu$M $Mn^{III}P$ and (B) 9 $\mu$M $Mn^{III}P(Dis)_2$. Buffer: 5 mM Tris-HCl, 50 mM NaCl, pH 7.

**Spectroscopic Studies.** The UV spectra of 9 $\mu$M $Mn^{III}P$ in the absence and in the presence of 18 $\mu$M distamycin (Figure 12) was practically the same, with the exception of the Dis absorption bands in the ultraviolet region. UV bands of distamycin at higher concentrations greatly overlap and distort $Mn^{III}P$ bands.

The absorption spectra of $Mn^{III}P$ (Figure 13A) shows hyperchromicity but no shift in the wavelength of maximum absorption upon addition of DNA as reported by Pasternack et al.[18] Figure 13B presents the changes in the spectra of $Mn^{III}P(Dis)_2$ in the presence of sonicated CT DNA. Addition of DNA also produced hyperchromicity in the Soret band (462 nm), but at 40 $\mu$M NP the increase in absorption was smaller than that of $Mn^{III}P$.

At this DNA concentration, distamycin absorption increased slightly. At 320 $\mu$M NP, the Soret band of $Mn^{III}P(Dis)_2$ increased to almost the same extent as that of $Mn^{III}P$, and distamycin absorption increased and its absorption peak shifted to 321 nm. This effect of CT DNA on the absorption peak of Dis has been reported previously.[30] This variation of the spectra in Figure 13B suggests that $Mn^{III}P$ and Dis moieties interact directly with DNA and that the final spectrum is a combination of the spectra of $Mn^{III}P$ and of distamycin in the presence of DNA.

## Discussion

Association of distamycin A with $Mn^{III}P$ was studied by electrochemical means. The mode of interaction is not known, but the fact that two distamycin molecules bind to $Mn^{III}P$ suggests axial ligation. This type of interaction is also supported by the inhibition effect of bound distamycin to the axial coordination of molecular $O_2$ and to its catalytic reduction. Experiments using DMF demonstrated that it is probably the oxygen atom of the formyl portion of the distamycin molecule that binds to $Mn^{III}P$.[31]

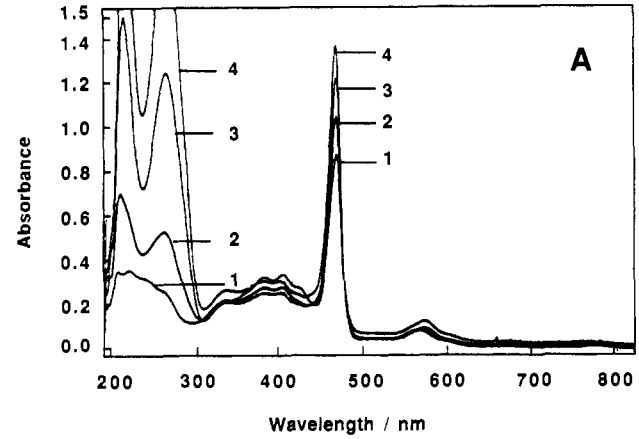


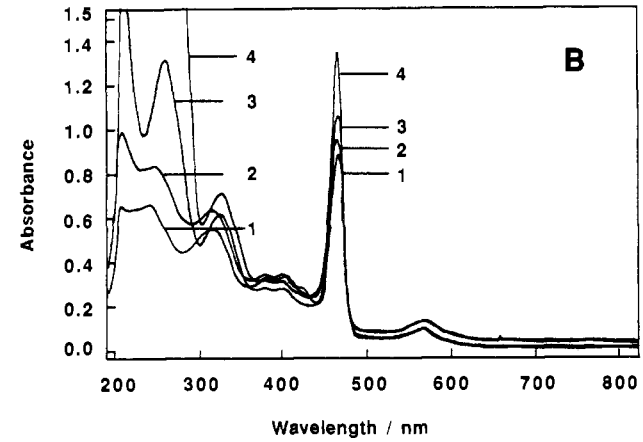


**Figure 13.** Visible spectra of (A) 9 $\mu$M $Mn^{III}P$ and (B) 9 $\mu$M $Mn^{III}P(Dis)_2$, (1) in the absence of DNA and in the presence of sonicated CT DNA with (2) 40 $\mu$M NP, (3) 160 $\mu$M NP, and (4) 320 $\mu$M NP. Buffer: 5 mM Tris-HCl, 50 mM NaCl, pH 7.

On the other hand, binding of distamycin did not affect the UV absorption spectra of $Mn^{III}P$.

The value of the binding constant, assuming a static equilibrium model, is somewhat larger than that reported for the coordination of two imidazoles to the tetraphenylporphine complex of Mn(III) in dichloromethane ($K = 6.29 \times 10^4$ $M^{-2}$)[32] and in dichloroethane ($2.8 \times 10^7$ $M^{-2}$),[33] of two pyridines to the mesophorphyrin IX complex of Mn(III) in water ($K = 0.1$ $M^{-2}$),[34] and of two imidazoles ($K = 3 \times 10^5$ $M^{-2}$) and two histidines ($2.5 \times 10^4$ $M^{-2}$) to $Fe^{III}P$ in water.[35]

Use of the mobile binding model gave an unsatisfactory fit to the amperometric titration data, probably because there is not interconversion during the measurement time between $Mn^{III}P$ and $Mn^{III}P(Dis)_2$, since Dis is tightly bound to $Mn^{III}P$. Thus, we propose that the static equilibrium model is probably more appropriate for this system.

The positive 23-mV shift in $E_p$ of Mn(III)P in the presence of excess distamycin suggests that distamycin binds more strongly to the reduced form of the manganese porphyrin by a factor of 2.5. Axial ligands generally interact more strongly with manganese(II) porphyrins than with manganese(III) porphyrins.[27,28]

The results of the titration of $Mn^{III}P(Dis)_2$ with sonicated CT DNA showed that adsorption and precipitation of the DNA complex occurs at a low ratio of [NP]/[$Mn^{III}P(Dis)_2$]. Precipitation of DNA by $Mn^{III}P(Dis)_2$ is a reversible process since addition of DNA to a solution with precipitate causes dissolution. This precipitation is probably the result of electrostatic neutralization of the negative charges of DNA by the positively charged complex. Exchange of $Na^+$ ions by this highly charged,

(30) Krey, A. K.; Hahn, F. E. *FEBS Letters* **1970**, *10*, 175.
(31) In recent preliminary experiments (B. Donovan and A. J. Bard) we have found that the oligopeptide netropsin, which is similar to distamycin but is terminated at both ends by amidine groups, does not interact with $Mn^{III}P$. This provides additional support to the proposal that it is the formyl group of distamycin that interacts with $Mn^{III}P$.
(32) Yuan, L.-C.; Bruce, T. C. *J. Am. Chem. Soc.* **1986**, *108*, 1643.
(33) Kelly, S. L.; Kadish, K. M. *Inorg. Chem.* **1982**, *21*, 3631.
(34) Taylor, J. H. *Biol. Chem.* **1940**, *135*, 569.
(35) Weinraub, D.; Peretz, P.; Faraggi, M. *J. Phys. Chem.* **1982**, *86*, 1839.

large complex caused DNA precipitation. At low DNA concentrations, a large number of Mn complex molecules will be bound to a given molecule of DNA, while, at higher DNA concentrations, the complex molecules are distributed among many DNA molecules. The change in the trend of the shift in $E_p$ of $Mn^{III}P(Dis)_2$ in the presence of different concentrations of DNA, for example, from positive potentials at low DNA concentrations to more negative values at higher DNA concentrations, indicates that the adsorption process dominates the electrochemical response, over the effect of binding to DNA, at the early stages of the titration. This occurs because adsorption and precipitation are present only at low DNA concentrations. Although we were unable to quantify the binding of $Mn^{III}P(Dis)_2$ to DNA, the binding site size was estimated to be about 15 bp. This value agrees with the arithmetic addition of the individual binding site sizes of $Mn^{III}P$ ($s$ = 3-4 bp)[1] and Dis ($s$ = 4-6 bp).[8-11]

The effect of DNA on the Soret band of $Mn^{III}P(Dis)_2$ complex was the same as that for $Mn^{III}P$ alone; however, the magnitude of the increase in the absorbance was greater for $Mn^{III}P$ at low NP concentrations. This may occur because the distamycin portion of the complex competes with the metalloporphyrin ring for sites in the double helix.

Comparison of the electrochemical and spectroscopic behavior of $Mn^{III}P$ and $Mn^{III}P(Dis)_2$ in the presence of DNA suggests that these two species associate with DNA in a similar fashion.

## Conclusion

In this paper we reported the binding of two DNA groove-binding molecules, $Mn^{III}P$ and Dis, by voltammetric methods. Two distamycin molecules bind one $Mn^{III}P$, probably by axial coordination of the oxygen atom of the formyl end to the Mn(III) center. Bis(distamycin) compounds are important, as shown by Dervan and others,[36-39] as potential recognition agents of large sequences of A-T rich DNA.

**Acknowledgment.** The support of this research by a grant from the National Science Foundation (CHE 8901450) is gratefully acknowledged.

(36) Dervan, P. B. *Science* **1986**, *232*, 464.
(37) Schultz, P. G.; Dervan, P. B. *J. Am. Chem. Soc.* **1983**, *105*, 7748.
(38) Younquist, R. S.; Dervan, P. B. *J. Am. Chem. Soc.* **1985**, *107*, 5528.
(39) Khorlin, A. A.; Krylov, A. S.; Grokhovsky, S. L.; Zhuze, A. L.; Zasedatelev, A. S.; Gursky, G. V.; Gottikh, B. P. *FEBS Lett.* **1980**, *118*, 311.

Contribution from the Department of Chemistry, Loyola University of Chicago, 6525 North Sheridan Road, Chicago, Illinois 60626, and Department of Chemistry and Center of Neurosciences of Coimbra, University of Coimbra, 3000 Coimbra, Portugal

# Physical Basis for the Resolution of Intra- and Extracellular $^{133}Cs$ NMR Resonances in $Cs^+$-Loaded Human Erythrocyte Suspensions in the Presence and Absence of Shift Reagents[§,‖]

Lisa Wittenkeller,[†] Duarte Mota de Freitas,*[,†] Carlos F. G. C. Geraldes,[‡] and Angelo J. R. Tomé[‡]

*Received September 5, 1991*

For human red blood cells (RBCs) loaded with $Cs^+$ and suspended in a shift reagent (SR) free medium, the extracellular $^{133}Cs^+$ NMR resonance was shifted upfield from the intracellular resonance. However, in the presence of the SRs $Dy(PPP)_2^{7-}$, $Dy(TTHA)^{3-}$, and $Tm(DOTP)^{5-}$ [where $Dy^{3+}$ and $Tm^{3+}$ denote dysprosium and thulium ions and $PPP^{5-}$, $TTHA^{6-}$, and $DOTP^{8-}$ represent the triphosphate, triethylenetetraminehexaacetate, and 1,4,7,10-tetraazacyclododecane-*N*,*N*′,*N*″,*N*‴-tetrakis(methylenephosphonate) ligands, respectively], the extracellular $^{133}Cs^+$ NMR resonance was shifted downfield from the intracellular resonance. The magnitudes of the $^{133}Cs^+$ shifts observed with $Tm(DOTP)^{5-}$ were much larger than those for $Dy(TTHA)^{3-}$ and $Dy(PPP)_2^{7-}$ at the same concentration. The direction of the $^{133}Cs^+$ shift induced by $Dy(PPP)_2^{7-}$ was the opposite of that previously reported for $^7Li^+$, $^{23}Na^+$, and $^{39}K^+$ NMR resonances. The negative sign of the pseudocontact $^{133}Cs$ shift induced by $Dy(PPP)_2^{7-}$ is related to the large size of the $Cs^+$ cation and its location in the equatorial region formed by the cone around the effective magnetic axis of the triphosphate SR. At physiologically relevant RBC concentrations, 2,3-diphosphoglycerate (DPG), of all intracellular phosphates tested, caused the largest $^{133}Cs^+$ shift. The $^{133}Cs^+$ resonance in carbonmonoxygenated RBC lysate shifted downfield by approximately 2.0 ppm with increasing hemoglobin concentration, whereas an increase in the diamagnetic susceptibility of the sample induced by hemoglobin is expected to induce an upfield shift of 0.1 ppm. The $^{133}Cs^+$ resonance was shifted downfield with increasing concentrations of two unrelated proteins, carbonmonoxyhemoglobin and lysozyme. We conclude that, in the absence of SRs, the physical basis for the resolution of intra- and extracellular $^{133}Cs$ NMR resonances in $Cs^+$-loaded human RBC suspensions arises from $Cs^+$ binding to intracellular phosphates, in particular DPG, and from the nonideality of intracellular water induced by hemoglobin.

## Introduction

Aqueous shift reagents (SRs) have been introduced in the past decade for the study of biologically important metal cations by nuclear magnetic resonance (NMR) spectroscopy.[1] Because of their high negative charges, SRs are not soluble in the interior of the lipophilic membrane and are repelled by the negatively charged head groups of phospholipids. Thus, SRs remain in the extracellular compartment during NMR experiments conducted on cell suspensions. With the use of SRs, the extracellular resonance is shifted away from the intracellular resonance, thus allowing the simultaneous observation of the two pools of metal ions. Information on metal cation transport and distribution in cell suspensions, and on enzymatic activity, is then easily obtained by metal NMR spectroscopy in the presence of SRs.[2,3]

In cell suspensions, the presence of SRs in the suspension medium leads to transmembrane differences in chemical shifts that result in resolution of intra- and extracellular $^7Li^+$, $^{23}Na^+$,

* To whom correspondence should be addressed.
† Loyola University of Chicago.
‡ University of Coimbra.
§ Presented in part at the Ninth Annual Meeting of the Society of Magnetic Resonance in Medicine, New York, August 1990.
‖ Abbreviations used in this paper: ADP, adenosine diphosphate; ATP, adenosine triphosphate; BMS, bulk magnetic susceptibility; COHb, carbonmonoxyhemoglobin; CORBC, carbonmonoxygenated red blood cell; deoxyRBC, deoxygenated red blood cell; $DOTP^{8-}$, 1,4,7,10-tetraazacyclododecane-*N*,*N*′,*N*″,*N*‴-tetrakis(methylenephosphonate); DPG, 2,3-diphosphoglycerate; Ht, hematocrit; NMR, nuclear magnetic resonance; $P_i$, inorganic phosphate; $PPP^{5-}$, triphosphate; PVP-100, poly(vinylpyrrolidone)-100; SR, shift reagent; $TTHA^{6-}$, triethylenetetraminehexaacetate.

(1) Sherry, A. D.; Geraldes, F. G. C. In *Lanthanide Probes in Life, Chemical, and Earth Sciences. Theory and Practice*; Bunzli, J.-C. G., Choppin, G. R., Eds.; Elsevier Press: Amsterdam, 1989; pp 93-126.
(2) Springer, C. S., Jr. *Ann. N.Y. Acad. Sci.* **1987**, *508*, 130.
(3) Kirk, K. *NMR Biomed.* **1990**, *3*, 1.

0020-1669/92/1331-1135$03.00/0 